Journal of Nuclear Materials 385 (2009) 236–241

Contents lists available at ScienceDirect

Journal of Nuclear Materials

journal homepage: www.elsevier.com/locate/jnucmat

Potential of direct metal deposition technology for manufacturing thick functionally graded coatings and parts for reactors components

L. Thivillon, Ph. Bertrand, B. Laget, I. Smurov *

Ecole Nationale d'Ingénieurs de Saint-Etienne (ENISE), DIPI Laboratory, 58 rue Jean Parot, 42023 Saint-Etienne cedex 2, France

ARTICLE INFO

PACS:
42.55.Lt
28.52.−s
68.35.−p
62.20.Fe
62.20.Qp
42.62.Cf

ABSTRACT

Direct metal deposition (DMD) is an automated 3D deposition process arising from laser cladding technology with co-axial powder injection to refine or refurbish parts. Recently DMD has been extended to manufacture large-size near-net-shape components. When applied for manufacturing new parts (or their refinement), DMD can provide tailored thermal properties, high corrosion resistance, tailored tribology, multifunctional performance and cost savings due to smart material combinations. In repair (refurbishment) operations, DMD can be applied for parts with a wide variety of geometries and sizes. In contrast to the current tool repair techniques such as tungsten inert gas (TIG), metal inert gas (MIG) and plasma welding, laser cladding technology by DMD offers a well-controlled heat-treated zone due to the high energy density of the laser beam. In addition, this technology may be used for preventative maintenance and design changes/up-grading. One of the advantages of DMD is the possibility to build functionally graded coatings (from 1 mm thickness and higher) and 3D multi-material objects (for example, 100 mm-sized monolithic rectangular) in a single-step manufacturing cycle by using up to 4-channel powder feeder. Approved materials are: Fe (including stainless steel), Ni and Co alloys, (Cu,Ni 10%), WC compounds, TiC compounds. The developed coatings/parts are characterized by low porosity (<1%), fine microstructure, and their microhardness is close to the benchmark value of wrought alloys after thermal treatment (Co-based alloy Stellite, Inox 316L, stainless steel 17-4PH). The intended applications concern cooling elements with complex geometry, friction joints under high temperature and load, light-weight mechanical support structures, hermetic joints, tubes with complex geometry, and tailored inside and outside surface properties, etc.

1. Introduction

Laser cladding is a surface processing technology involving the deposition of a material of a different nature on a metal substrate using a laser beam [1–4]. This flexible technique allows cladding consumables to be deposited in either wire or powder form transported by an inert gas and then injected into the molten pool either laterally or coaxially to the laser beam. This technique can be used on both new and worn components and is typically used to rebuild worn or damaged surfaces and to hard-face wear, corrosion or oxidation susceptible materials.

Conventional repair techniques such as tungsten inert gas (TIG), metal inert gas (MIG) and plasma welding are characterized by a large temperature increase in the workpiece, re-crystallization, and weakening of the base alloy due to a wide temperature distribution over the working area. Contrary to these methods, heat transfer in the DMD laser cladding that typically uses a 0.5 – 3.0 mm diameter laser beam occurs in localized areas. As a result, the heat-affected zone and residual stresses are reduced and therefore a lower part distortion and better mechanical characteristics are achieved. A great variety of materials may be processed by laser cladding including those generally considered unweldable by conventional methods as, for example, Fe – Cr system may be used in the nuclear industry applications. Main characteristics of the coating deposition techniques are compared in Table 1.

Integration of laser cladding technology with computer-aided manufacturing and design (CAD/CAM), robotics, sensors, and control devices allows layer-by-layer manufacturing of components with complex geometry in a one-step process [5–7]. For example, thin-walled parts with a high aspect ratio for nuclear applications can be directly fabricated. Such components are light-weight without loss of structural strength and cool rapidly due to their greater surface area-to-weight ratio. DMD technology can diminish the overall production cost because of manufacturing and machining time savings [3].

In the present study TIG- and DMD-deposited coatings from Co-based Stellite 6 and Ni- superalloy Inconel 625 are analyzed. The coating quality is characterized by several parameters such as microstructure, microhardness distribution, and dilution. The

* Corresponding author. Tel.: +33 477437561; fax: +33 477743497.
E-mail address: smurov@enise.fr (I. Smurov).

0022-3115/$ - see front matter © 2008 Elsevier B.V. All rights reserved.
doi:10.1016/j.jnucmat.2008.11.023

Table 1
Main characteristics of coatings deposited by different techniques.

Parameters	Laser cladding	MIG	TIG	Plasma welding
Thickness (mm)	0.2 – 2	1 – 6	0.5 – 3.0	1 – 5
Deposition rate (kg h^{-1})	0.2 – 7	2.3 – 11	0.5 – 3.5	2.5 – 6.5
Distortion (–)	Low	Medium	High	Medium
Dilution (%)	1 – 5	15 – 20	10 – 20	Medium

relations between the employed DMD manufacturing strategies and the geometrical and mechanical characteristics of the built objects are discussed.

2. Experimental set-up

The laser cladding experiments were performed on a Trumpf DMD505 machine equipped by a 5 kW continuous wave CO_2 laser system. A nozzle mounted on a five-axis gantry transports the powder coaxially to the laser beam onto the molten pool created on the workpiece surface. Two computer-controlled powder feeding systems (up to 4 powders applicable) can operate simultaneously for powder mixing *in situ*. A *POM, Inc.* system equipped with 3 CCD cameras monitors the clad dimensions. The output from these cameras is digitized to control the current size of the molten pool via comparison with the specified one and then regulating the laser power if this parameter has gone beyond the specification [8].

3. Coating

3.1. Experimental

Commercial metal powders Co-based Stellite 6 and Ni-superalloy Inconel 625 by TLS Technick GmbH&Co (Bitterfeld) with+45 – 100 μm particle size were laser-cladded on a substrate from S235 steel. The chemical compositions of the materials used in the experiments are presented in Table 2. Ni-superalloy Inconel 625 and Co-based alloy Stellite 6 were deposited by DMD with laser cladding speed $S = 1000$ and 1500 mm min^{-1}, laser power $P = 4000$ and 3000 W, respectively. Laser spot D of 3 mm and powder feeding rate F of 63 g min^{-1} were kept fixed. A triple clad layer was produced by overlapping individual laser tracks by 1.5 mm in each step. In order to compare DMD and TIG coatings, a triple layer from the above-mentioned materials was produced by TIG with current 150 A and voltage 13 V. Filler rod of 1 mm diameter was automatically fed to the front edge of the weld pool. In the DMD and TIG experiments an argon – helium mixture was employed as shielding gas. Microstructures of the coatings built up by the two methods were analyzed by optical microscopy using an Olympus BH-2.

3.2. Results and discussion

Fig. 1 shows the microhardness distribution of the coatings from Ni-superalloy Inconel 625 deposited by TIG and DMD processes. At a first sight, one may note a shorter transition zone and a higher microhardness of the DMD-deposited coating in comparison with the conventional TIG-deposited one. The average microhardness of Ni-superalloy Inconel 625 cladded by DMD is about 2697 MPa and is 30% greater than that of the TIG-deposited material. The weakened zone is clearly visible on the TIG microhardness curve. A wide temperature distribution over the working area during the weld metal deposition by TIG caused a great heat input. It resulted in a large heat-affected zone (HAZ), partial recrystallization of the cladded alloys and their weakening. Microhardness decreases by 7% to reach about 1893 MPa. As to the laser-cladded coatings, no weakening was observed.

Metallographic analysis of the DMD and TIG coatings demonstrates a finer grain microstructure of the DMD one (Fig. 2).

Table 2
Chemical composition (wt%) of Ni-superalloy Inconel 625 and Co-based alloy Stellite 6.

Material	C	Si	Cr	Mn	Fe	Co	Ni	Nb	Mo	W
Ni-superalloy Inconel 625	–	0.394	21.59	0.44	4.52	0.199	Bal.	2.95	9.08	–
Co-based alloy Stellite 6	0.78	0.679	28.99	0.21	2	Bal.	1.49	–	1.1	4.5

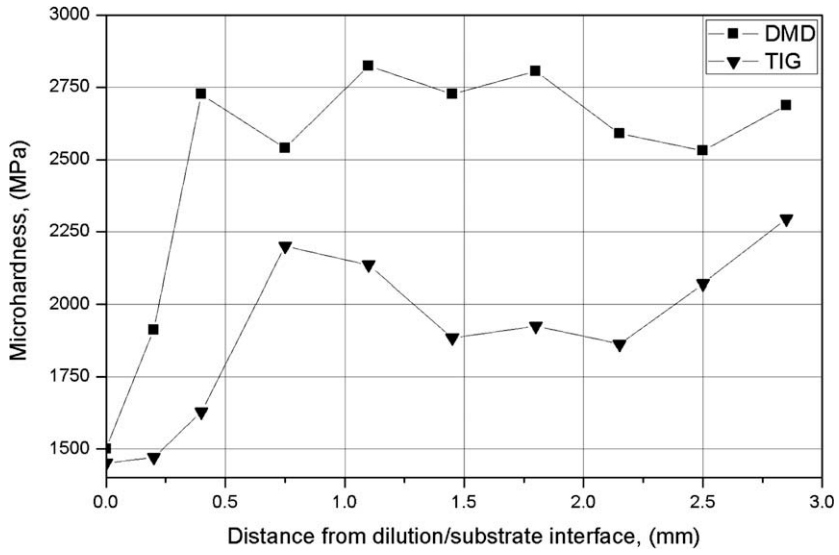

Fig. 1. Microhardness of Ni-superalloy Inconel 625 coatings deposited by DMD and TIG techniques at different distances from the substrate/coating interface. Deposition parameters: (i) for DMD, $P = 4000$ W, $S = 1000$ mm min^{-1}, $d = 3$ mm, $F = 63$ g min^{-1}, step is 1.5 mm; (ii) for TIG, $I = 150$ A, $V = 13$ V, filler rod diameter is 1 mm.

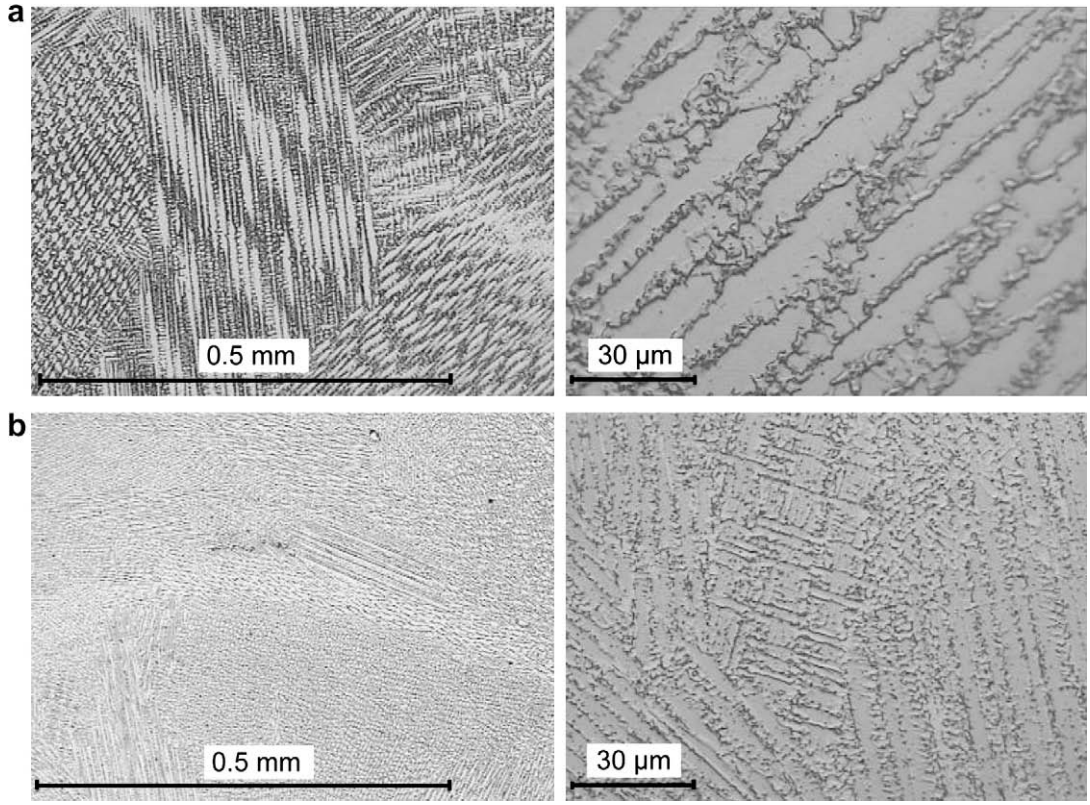

Fig. 2. Microstructure of Ni-superalloy Inconel 625 coatings deposited by (a) TIG and (b) DMD.

This phenomenon is explained by a high nucleation rate combined with slow growth. The grain size d_g is described by the following expression:

$$d_g = 1.1\left(\frac{R}{n}\right)^{3/4} \quad (1)$$

where n ($s^{-1}\,cm^{-3}$) is the nucleation rate and R ($mm\,s^{-1}$) is the nucleus growth rate.

The grain size and its internal structure can change depending on the cooling rate. Nucleus quantity is small at a small value of supercooling (slow cooling rate). Under this condition big grains are formed as shown on the example of the TIG-deposited coating in Fig. 2(a). Laser cladding is characterized by a high cooling rate. The nucleation rate increases with the supercooling value (high cooling rate) while the grain size reduces in the solidified metal as can be seen in the micrograph of the DMD coating (Fig. 2)(b)). It is known that the grain size of a metal influences its mechanical properties such as tensile strength, ductility, and microhardness. For a number of applications, coatings with a fine grain microstructure are preferable. Failure mechanism in such coatings is different because micrograin structure hinders cracks formation. As a practical consequence, enhanced plasticity for a given hardness may be reached. Typically, micrograin-size materials are more oxygen-corrosion resistant. As a potential consequence, one can predict improved neutron-swelling resistance.

Fig. 3 shows a typical cross-section of the Co-based alloy Stellite 6 coatings produced by the two techniques. The average microhardness of the DMD coating is about 5100 MPa, which is 1.4 times greater compared to the TIG one. It is interesting to note that the DMD coating has excellent metallurgical contact with the substrate although the dilution zone is absent (Fig. 3(b)). In contrast, the depth of the melted substrate material t for TIG is irregular and 0.7 mm on average for the given operational parameters

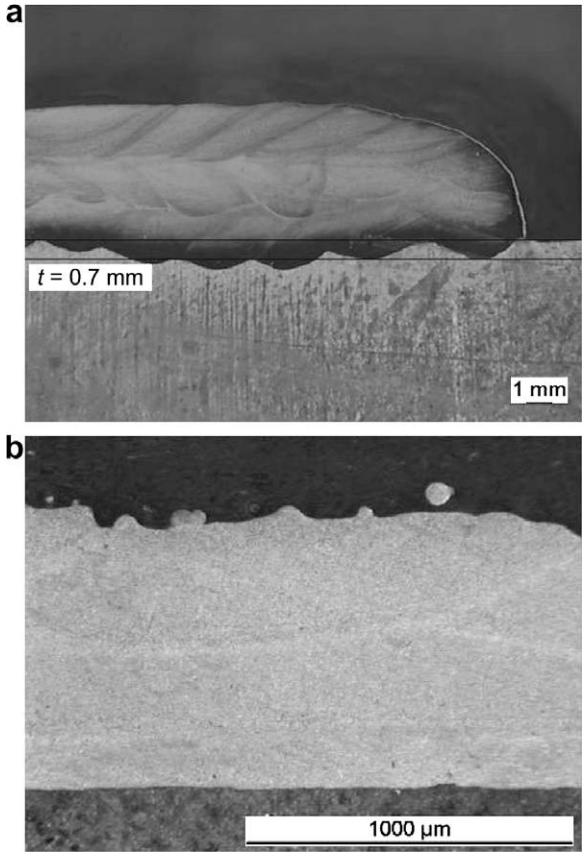

Fig. 3. Cross-sections of Stellite 6 triple layers from built-up by (a) TIG and (b) DMD techniques. Deposition parameters: (i) for DMD, $P = 3000$ W, $S = 1500$ mm min^{-1}, $d = 3$ mm, $F = 63$ g min^{-1}, step is 1.5 mm; (ii) for TIG, $I = 150$ A, $V = 13$ V, filler rod diameter is 1 mm.

Table 3
Chemical composition (wt%) of Ni-superalloy Inconel 718 and stainless steel 17-4PH alloy.

Material	C	Al	Si	Cr	Mn	Fe	Co	Ni	Cu	Mo	Nb
Ni-superalloy Inconel 718	0.037	0.49	0.03	18.06	0.03	17.89	0.07	Bal.	<0.1	2.95	5.16
Stainless steel 17-4PH	0.035	–	0.55	16.2	0.32	Bal.	–	3.5	4.1	0.09	–

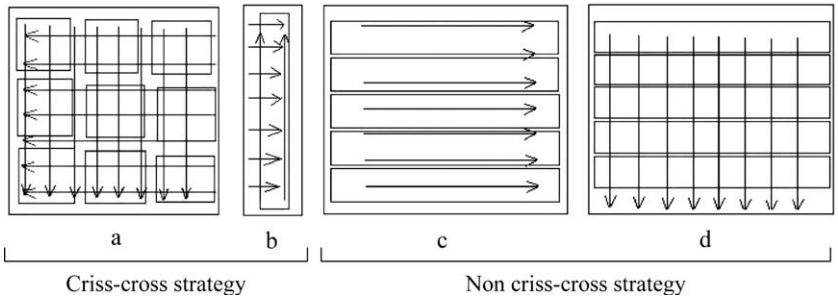

Fig. 4. Criss-cross and non criss-cross manufacturing protocols applied to produce 3D objects. Location of the test specimens for the tensile test is shown by rectangles.

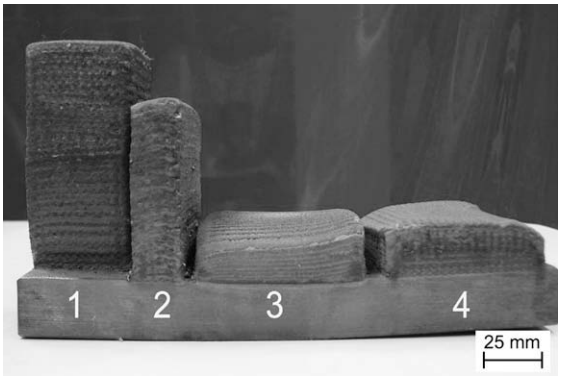

Fig. 5. 3D objects formed from stainless steel 17-4PH alloy fabricated by DMD employing (1, 2) criss-cross and (3, 4) non criss-cross manufacturing strategies. Deposition parameters: $P = 5000$ W, $S = 900$ mm min^{-1}, $d = 5.5$ mm, $F = 32$ g min^{-1}, step is 3 mm.

(Fig. 3(a)). This is caused by the stochastic nature of the electric arc used in TIG.

The performed experiments confirmed that, contrary to the TIG-deposited coatings, the laser-cladded coatings are characterized by minimal dilution, excellent adhesion, and enhanced mechanical properties.

4. Rapid prototyping

4.1. Experimental

Several samples were produced to study the effect of the manufacturing strategy on the part geometrical and mechanical characteristics. Commercially available metal powder stainless steel 17-4PH and Ni-superalloy Inconel 718 by TLS Technick GmbH&Co (Bitterfeld) with +45 – 100 μm particle size were used. Their chemical composition is presented in Table 3. The criss-cross and non

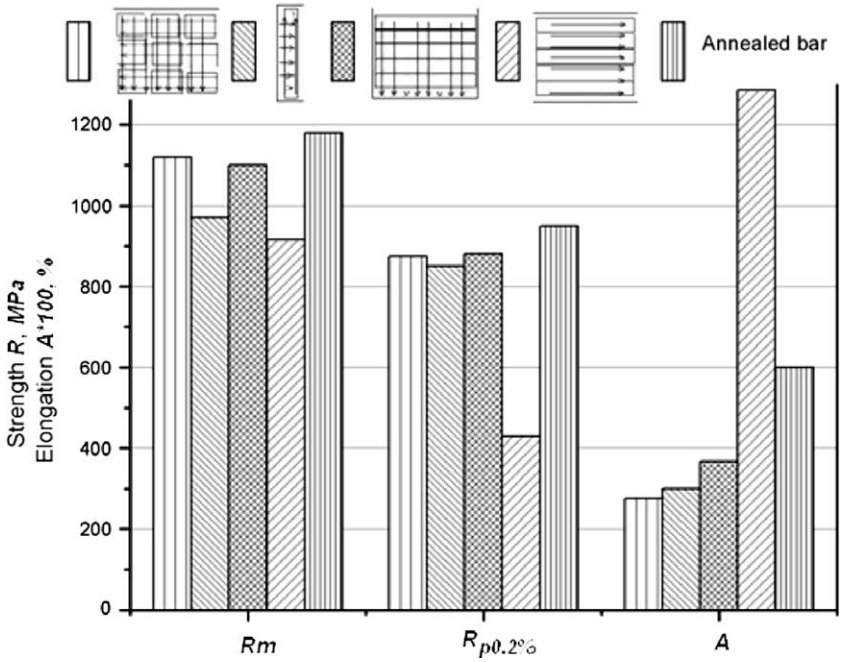

Fig. 6. Dependence of the ultimate tensile strength R_m (MPa), the yield strength $R_{p0.2\%}$ (MPa) and the elongation A (%) of the DMD-deposited stainless steel 17-4PH alloy on the manufacturing strategies.

criss-cross manufacturing strategies were applied to fabricate four samples from stainless steel 17-4PH alloy, i.e. cladding directions of two consecutive layers were perpendicular to one another (criss-cross strategy) or parallel (non criss-cross strategy) (Fig. 4). In these experiments the POM control system was deactivated to reveal the peculiarities of each strategy.

After evaluating the influence of the manufacturing strategy on the sample's geometrical characteristics, some specimens were manufactured and machined and then tested on a tension testing machine. The test specimens were mounted as follows:

- for the criss-cross strategy: perpendicular (Fig. 4(a)) and parallel (Fig. 4(b)) to the plate;
- for the non criss-cross strategy: parallel (Fig. 4(c)) and perpendicular (Fig. 4(d)) to the cladding direction.

A sample of Ni-superalloy Inconel 718 was fabricated by criss-cross manufacturing strategy and subjected to metallographic analysis by optical microscopy using an Olympus BH-2.

4.2. Results and discussion

Fig. 5 shows multilayer objects fabricated by different manufacturing strategies. Samples 3 and 4, built-up by non criss-cross strategies, are uneven in height compared to samples 1 and 2, fabricated by criss-cross strategies. They are saddle-like, i.e. the ends and middle of each layer are different in height, and the height varies in the direction perpendicular to the cladding direction.

The first effect is caused by acceleration and deceleration of the coaxial nozzle in the beginning and at the end of the continuous path and, consequently, by variation of the cladding speed (specific energy) between the ends and the middle of a layer. The specific energy E (J mm^{-2}) is given by the expression:

$$E = \frac{P}{D \cdot S} \tag{2}$$

where P (W) is the laser power, D (mm) is the laser spot diameter, and S (mm s^{-1}) is the cladding speed (speed of the nozzle movement relatively to the substrate). The specific energy increases dramatically at both ends due to a lower scanning velocity. As a result, a hole forms in the middle of the cladded track. Therefore, the appropriate specific energy should be defined to achieve a uniform layer-by-layer deposition (e.g. the optimal specific energy for parts from nickel alloys is 100 – 200 J mm^{-2} [9]).

Variation of the height in the direction perpendicular to the cladding direction is caused by the clad superposition. The first and the last clads of a layer border with other clads only at one side; that is not the case for the inside clads. Thus, the laser-molten metal spreads differently on the layer surface at the borders versus inside the sample, bringing about the height variation. The height error accumulating from layer to layer results in a curved upper surface of the part. It may be possible to reduce this effect by decreasing the height/width ratio:

$$H < \frac{L}{4} - \frac{L}{5}. \tag{3}$$

In order to eliminate the height error, the *criss-cross manufacturing strategy* is applied. Multilayer samples 1 and 2 with regular height are presented in Fig. 5.

Results of the tensile test of the specimens fabricated from the above-mentioned samples are presented in Fig. 6. The dependence of the mechanical properties on the manufacturing strategy is evident. Although the DMD-deposited stainless steel 17-4PH alloy possesses an improved microstructure with a significantly reduced grain size, its mechanical properties are slightly worsened. The best mechanical characteristics of the components are achieved by employing the criss-cross DMD manufacturing strategy. The ultimate tensile strength R_m of 1120 MPa and the yield strength $R_{p0.2}$ of 880 MPa are approximately 6 and 7% less than those of the annealed stainless steel 17-4PH alloy, respectively. The

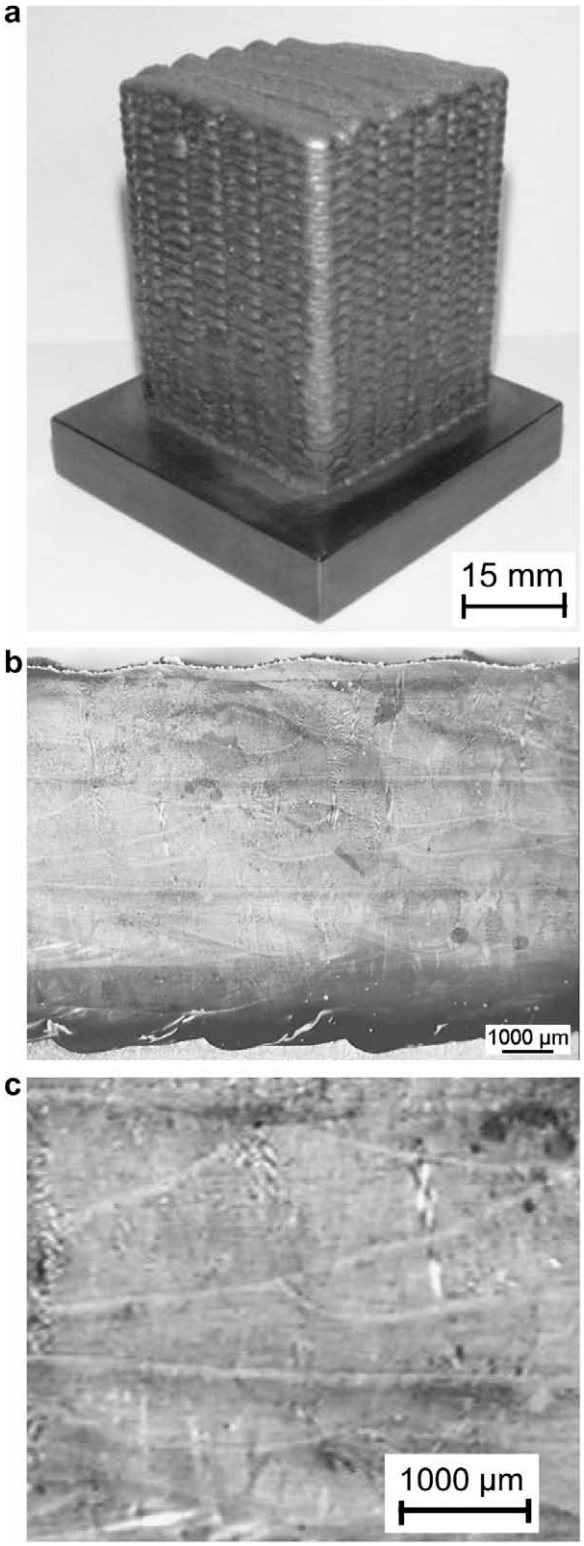

Fig. 7. (a) 3D object from Ni-superalloy Inconel 718 by DMD employing a criss-cross manufacturing strategy when the cladding directions in two consecutive layers are perpendicular; (b) clad realised by several passes; (c) clad macrostructure: interfaces between individual cladded lines are visible. Deposition parameters: P = 5000 W, S = 825 mm min^{-1}, F = 56 g min^{-1}, d = 5.5 mm, step is 3 mm.

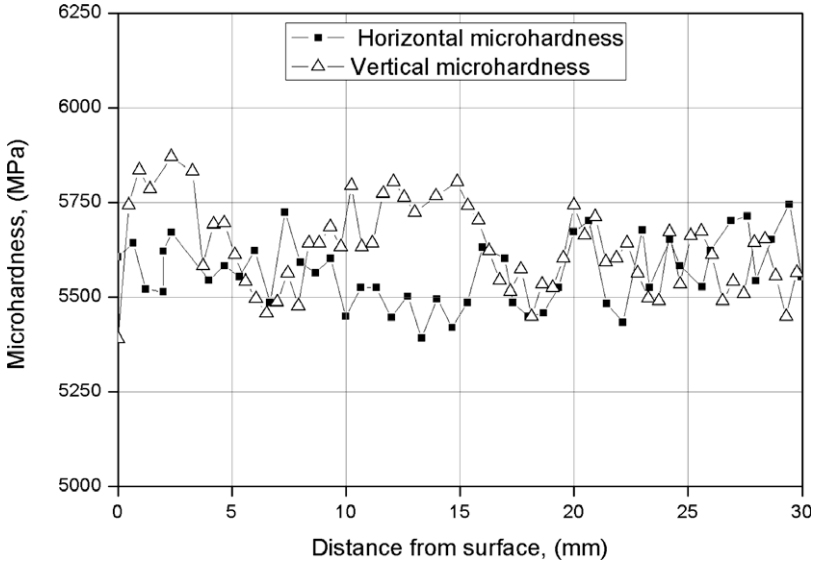

Fig. 8. Vertical and horizontal microhardness of 3D objects (Inox AISI 431) measured at different distances from the substrate surface. Deposition parameters: $P = 5000$ W, $S = 1000$ mm min^{-1}, $d = 5.5$ mm, $F = 72$ g min^{-1}, step is 3 mm.

elongation value of A (%) in the cladding direction is about twice that of the annealed stainless steel 17-4PH alloy.

One of the factors that decrease the quality of the manufactured parts is the accumulation of residual stresses due to an unbalanced heating of the surface. Therefore it is important to select an appropriate path aiming to reduce this effect and increase mechanical characteristics of the parts.

According to the studies reported in the literature [10], reducing the number of layers by increasing the height of the deposited layers can improve mechanical proprieties of the resulting component. However, the accuracy of the built-up parts, and particularly of those with complex geometry, may diminish when the layers become higher. Therefore, a compromise should be found, taking into account the geometry of the manufacturing component.

Metallurgical examination of the DMD sample's cross-section revealed visible interfaces between individual cladded lines (Fig. 7). The most probable explanation of this may be the interaction of the solidifying molten pool with the ambient gas atmosphere resulting in the formation of thin oxide layers. Microhardness measured vertically and horizontally is practically the same, which indicates a uniform microstructure of the multilayer sample (Fig. 8).

5. Conclusion

Today laser cladding, in particular its industrial version DMD, represents the most rapidly growing field of the industrial laser surface treatment: cladding of Co-based alloy stellite is a common service proposed by laser job shops. Properties and performance of the DMD coatings are superior compared to the conventionally deposited TIG ones. The actual trend is to apply a wide range of powders that are already used in thermal spraying as well as the ones specially designed for laser cladding. Up-grading DMD technology for fabrication of multi-component and graded coatings is the objective of intensive research. Application of DMD for the direct manufacturing of near-net-shape metal parts of a size of several tens of cm is a further stage of its evolution.

Acknowledgement

The tension tests were carried out by SETIM (France).

References

[1] John C. Ion, Laser processing of Engineering Materials: principles, procedure and industrial application, Elsevier Butterworth-Heinemann, Burlington, MA, 2005.
[2] William M. Steen, Laser Material Processing, third Ed., Springer, London, 2003.
[3] E. Toyserkani, A. Khajepour, S. Corbin, Laser Cladding, CRS Press, Boca Raton, Florida, 2005.
[4] J. Th. M. De Hosson, V. Ocelik, Functionally graded materials produced with high power lasers, Proceedings of ASTRA-2003, Hyderabad, India, 2003, pp. 368 – 376.
[5] I. Yadroitsev, Ph. Bertrand, B. Laget, I. Smurov, J. Nucl. Mater. 362 (2007) 189.
[6] W. Lengauer, K. Dreyer, J. Alloys Comp. 338 (2002) 194.
[7] Terry Wohlers, Wohlers Report 2005, Rapid Prototyping, Tooling & Manufacturing State of the Industry, Annual Worldwide Progress Report.
[8] The POM Group Inc., Auburn Hills, Michigan, USA, 2008 June, in Internet www.pomgroup.com.
[9] L. Peng, Y. Taiping, L. Sheng, L. Dongsheng, H. Qianwu, X. Weihao, Z. Xiaoyan, Intern. J. Machine Tools & Manufacturing 45 (2005) 1288.
[10] K. Ramaswami, Process planning for shape deposition manufacturing, PhD thesis Stanford University, 1997.